DESIGNING AIRCRAFT TRAFFIC FLOWS USING DATA-DRIVEN QUEUING MODELS

Eri Itoh[1,2], Furuto Kato[2], Koki Higasa[2] & Michael Schultz[3]

[1]Air Traffic Management Department, Electronic Navigation Research Institute
[2]Department of Aeronautics and Astronautics, The University of Tokyo
[3]Institute of Logistics and Aviation, Technische Universität Dresden

Abstract

This paper proposes a scientific and systematic method for designing future air traffic management systems by integrating data science, theoretical modeling, and simulation evaluation. Also, it presents a part of a case study focusing on the data-driven and theoretical modelings of arriving traffic flow in airports. A stochastic data analysis was conducted using actual radar tracks and flight plans before the impacts of COVID-19, where the queuing model parameters were estimated based on the conducted analysis. The proposed data-driven modeling approaches contribute to the analysis of the bottlenecks in air traffic and to their solutions. Overall, we believe that the outcomes of this study provide insights on future operational strategies and system designs, which can realize more efficient air traffic management systems.

Keywords: data science, queuing theory, theoretical modeling, system design, air traffic management

1. Introduction

One of the most important requirements for designing future air traffic management (ATM) systems is to accommodate global air traffic growth while improving efficiency and safety. It is also necessary to mitigate traffic congestion and delay time and reduce environmental impacts. The estimation of future air traffic increments is now challenging because of the impacts of COVID-19; however, passenger and cargo movements are expected to significantly increase on a long-term basis.

In this study, the authors aimed to establish a scientific and systematic method of designing future ATM systems by integrating data science, theoretical modeling, and simulation evaluation. In one of the authors' works [1], the best strategies of shifting arrival flow control to time-based management were analyzed based on stochastic data analyses. Also, the succeeding studies [2–4] applied the queuing theory to model arrival traffic flow in a case study involving Tokyo International Airport. The parameters of the queuing models were estimated by stochastic data-driven analysis using two years of radar track and flight plan data. The outcomes of these studies clarified how to improve aircraft arrival control strategies. These theoretical modeling approaches also recommended scenarios to be further analyzed using simulation studies, and the proposed operational strategies were quantitatively clarified through fast-time simulation validation [5]. The data-driven and queue-based modelings were applied to a case study involving Singapore Changi International Airport [6]. Overall, analyzing the different features of the arrival processes in the case study airports provided insights that helped in better understanding arrival control strategies and in establishing systematic approaches for designing arrival management systems for the long-range traffic flows [7].

Several studies have analyzed aircraft arrival traffic flow using the queuing theory. Aircraft arrival delay was analyzed in [8–11] by employing queuing models that especially focused on runway-related delay and capacity constraints. However, in their case studies, the authors did not make use of operational data or compare their results with actual data. In the authors' studies [2, 3], based on the analyses of actual data, a $G/G/c$ queuing model was designed to analyze air traffic in the airspace around an airport. In [4], a macroscopic analysis of the aircraft arrival traffic at an airport was conducted using a classical $M/G/c/K$ queuing model. In this paper, a data-driven queuing approach was
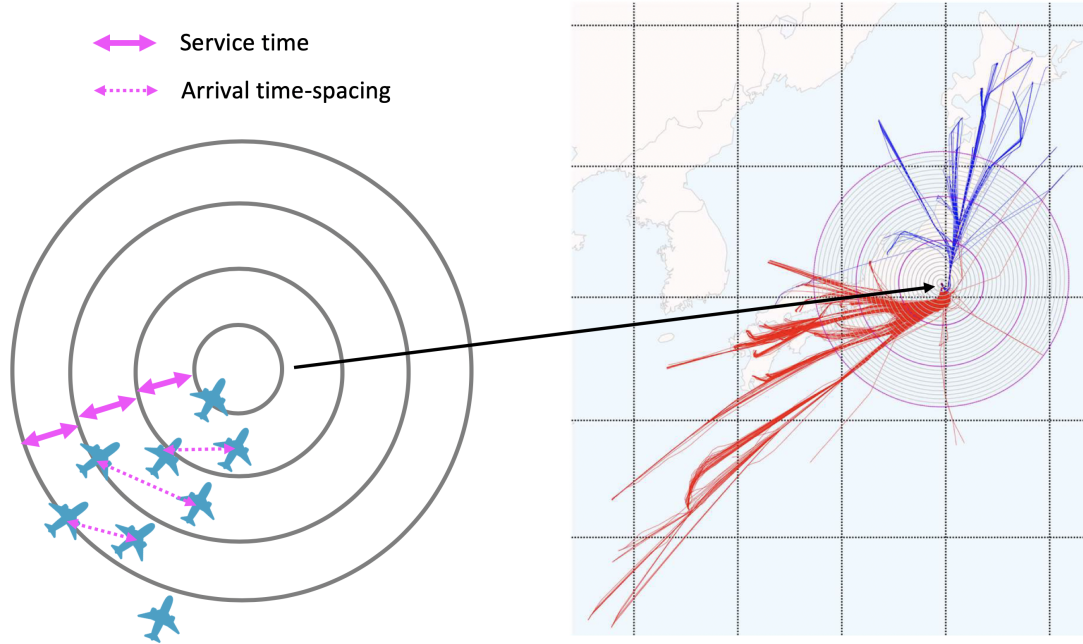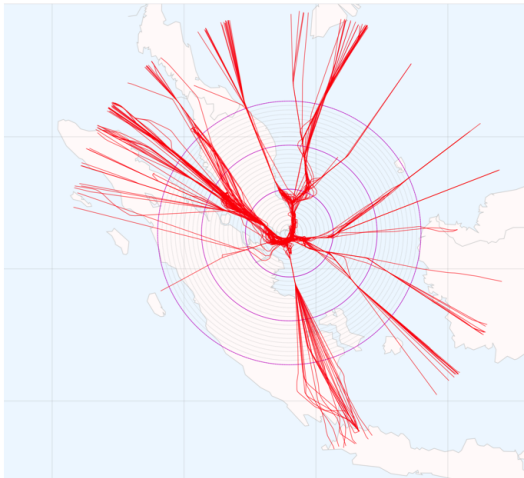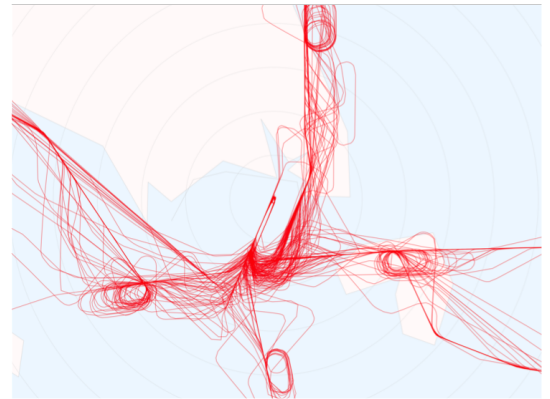
Figure 1. One-day examples of the arriving flight track data at Tokyo International Airport within a 300-NM radii concentric circle centered at the airport and an illustration of the service time and interarrival time (arrival time-spacing) using circles [2].

[1] Arrival tracks within a 300 NM radii concentric circle centered at the airport.

[2] Arrival tracks around Singapore Changi International Airport (emphasizing the holding areas).

Figure 2. One-day examples of the arriving flight track data at Singapore Changi International Airport [6].

introduced, and its contribution to designing operational strategies and ATM systems was reviewed by focusing on aircraft arrival traffic management. Furthermore, the impacts of point-merge (PM) operation, which have been implemented in the arrival routes at Tokyo International Airport, were discussed based on the proposed approach.

The rest of this paper is organized as follows. Section 2 describes data-driven and queue-based modeling approaches for aircraft arrival traffic flows. Section 3 reviews the analytical results of applying the data-driven queuing models of the arrivals at Tokyo International Airport and Singapore Changi International Airport [6] and compares the operational strategies at the case study airports. Section 4 focuses on the PM operation at Tokyo International Airport, which has been implemented in July 2019, and discusses the effectiveness of the PM implementation based on an analysis using the proposed approach. Finally, Section 5 provides conclusions and outlines our plans for future work.

2. Data-driven queuing model
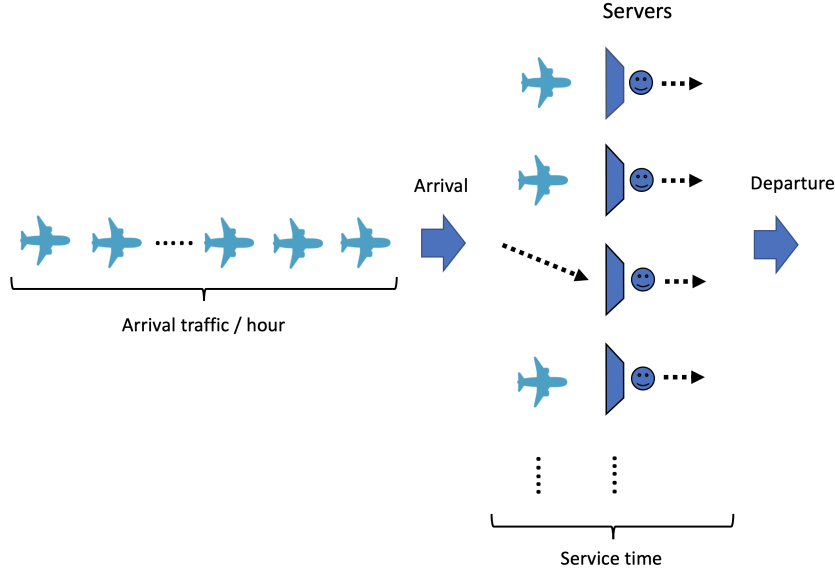
2.1 Model description

Figure 3. Queuing model example for aircraft arrival traffic.

Conventional studies indicated that the characteristics of arrival traffic processes depend on the distance and/or flight time at destination airports [1, 7].

By focusing on the two case study airports (Tokyo International Airport and Singapore Changi International Airport), the characteristics of the arrival traffic flows were analyzed based on data-driven queuing models [2–4, 6]. An airspace area of radius 300 NM (centered at the airport) around the airport was partitioned using concentric circles (see Fig. 1 and 2), with radii at increments of 10 NM. This partitioning defined 29 airspace areas $i = 1, 2, ..., 29$, where airspace $i = 1$ is the area around the airport in the circular ring defined by the 10 and 20 NM radii, airspace $i = 2$ is the area around the airport in the circular ring defined by the 20 and 30 NM radii, and so on.

Concerning the partitioned airspace $i \in \{1, 2, \ldots, 29\}$, the time between two consecutive arrivals entering the airspace i (crossing the bigger concentric circle) is called the aircraft inter-arrival time. Upon arrival, the aircraft receives a service time at airspace i, which is the time the aircraft spends flying the airspace i. This way, the distance-based arrival process is considered as a multi-server queuing model in which the number of servers indicates the number of aircraft that are allowed to be present at any time in the given airspace i, meaning that the capacity of the airspace i. Fig. 3 explains the formulation of the queuing model at each airspace i. Each specific airspace is independently analyzed.

2.2 $G/G/c$ queuing model

Here, we apply a multi-server queuing model to each disjoint airspace area $i \in \{1, 2, \ldots, 29\}$. Then, the aircraft arrival process can be formulated through a $G/G/c$ queuing model [2].

Let D_i denote the delay an aircraft experiences in the airspace area i. Then, we approximate the total airborne delay in the airspace area i as follows:

$$\mathbb{E}[D_i^{G/G/c}] \simeq \mathbb{E}[D_i^{M/M/c}] \frac{C_{A_i}^2 + C_{B_i}^2}{2}, \tag{1}$$

where $C_{A_i} = \frac{\sigma[A_i]}{\mathbb{E}[A_i]}$ is the coefficient of variation of the aircraft inter-arrival time in the airspace area i, and $C_{B_i} = \frac{\sigma[B_i]}{\mathbb{E}[B_i]}$ is the coefficient of variation of the aircraft service time in the airspace area i. Here

$\mathbb{E}[A_i]$ and $\sigma[A_i]$ are the mean and standard deviations of the aircraft inter-arrival time, and $\mathbb{E}[B_i]$ and $\sigma[B_i]$ are the mean and standard deviations of aircraft service time in the airspace area i.

In Eq. (1), $\mathbb{E}[D_i^{M/M/c}]$ denotes the expected aircraft delay time in the airspace area i when the $M/M/c$ queuing model is considered, which is well known [12, 13]. This means that the arrival process is considered as a Poisson process with a parameter λ_i, where the service times are assumed to follow an exponential distribution with a parameter μ_i, and there is also a fixed number of parallel servers c_i. Moreover, for stability, we have

$$\rho_i = \frac{\lambda_i}{c_i \cdot \mu_i} < 1. \tag{2}$$

If ρ_i is not lower than 1, then the queue becomes unstable, and the estimated delay time for incoming aircraft tends to become extraordinarily long.

3. Operational strategies at the case study airports

3.1 Data description

This section focuses on the aircraft arrival operation at a runway during the most congested time periods and reviews the analytical results of the different operational features at the two case study airports [2, 3, 6].

As one of the case studies, this section covers the arriving air traffic from the southwest direction at runway 34L of Tokyo International Airport. One-day examples of flight track data are shown in Fig. 1. The statistical and stochastic features of the aircraft arrival data were analyzed using flight plans and track data of 71 days that were selected from odd months of 2016 and 2017. The data covers all the nominal operations at Tokyo International Airport except for weather impacts and other rare events. The most congested periods occurred between 17:00 and 22:00. Air traffic flow in Japan is controlled, with a central focus on arrivals at Tokyo International Airport. The maximum total number of arrivals was 40, including 30 from the southwest and 10 from the north. The arrivals from the southwest normally arrived at a runway that is only used for arrival traffic during peak periods.

Another case study used ADS-B data of arrival flight tracks (total 110 days from March to September) of 2019 at Singapore Changi Airport [7]. The ADS-B data covered most of the flights under instrument flight rules and captured essential characteristics of the incoming traffic flow. Excluding the day traffic under non-nominal operation (extremely small number of traffic in a day), the arrival traffic data was interpolated every second and used in the analysis. Fig. 2 shows an example of the arrival one-day track data at Changi International Airport within a 300 NM radii concentric circle centered at the airport. Concentric circles every 10 NM from 10 NM to 300 NM radii were drawn, as shown in the figure. The most congested period occurred between 10:00 AM and 24:00. International flights arrive at the airport from all over the world, and the flights from the ASEAN region hold the largest share.

3.2 Stochastic features in the arrival processes

First, the stochastic features of the aircraft traffic flow arriving at Tokyo International Airport were analyzed based on the data distributions of the service times and inter-arrival times. Fig. 4 shows the empirical distribution of the service times corresponding to the airspace $i \in \{1, 3, 9, 19\}$ with Gaussian fitting. As shown in Fig. 4, the Gaussian distribution well approximated the service time distribution. This comparison of the service time at each airspace i emphasizes the strategies that the air traffic controllers used for the arrivals at Tokyo International Airport. One of the most significant strategies is illustrated in the service time distribution of the airspace $i = 3$, and it corresponds to the airspace between the concentric circles of radii 30 and 40 NM. This is explained by the fact that arrival time-spacing was actively conducted by air traffic controllers in the airspace between the concentric circles of radii 30 and 40 NM, just before the aircraft entered the terminal area.

Fig. 5 shows the empirical probability densities of the aircraft inter-arrival time corresponding to the airspace $i \in \{1, 3, 9, 19\}$ with their exponential fittings. As shown in Fig. 5, the data-driven analysis clarifies that the empirical distribution of the inter-arrival time was well approximated by an exponential distribution where the arriving aircraft flew beyond the 150 NM circle in a case study at Tokyo
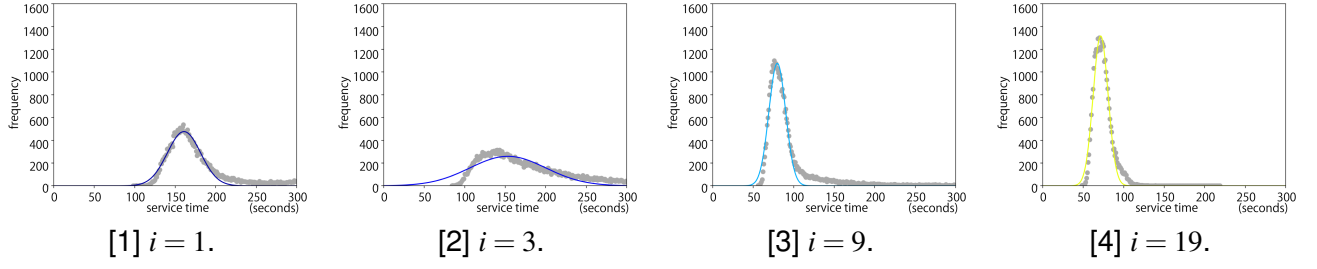
[1] $i = 1$.   [2] $i = 3$.   [3] $i = 9$.   [4] $i = 19$.

Figure 4. Distribution of the service times with Gaussian fitting targeting the arrivals at Tokyo International Airport. [2]

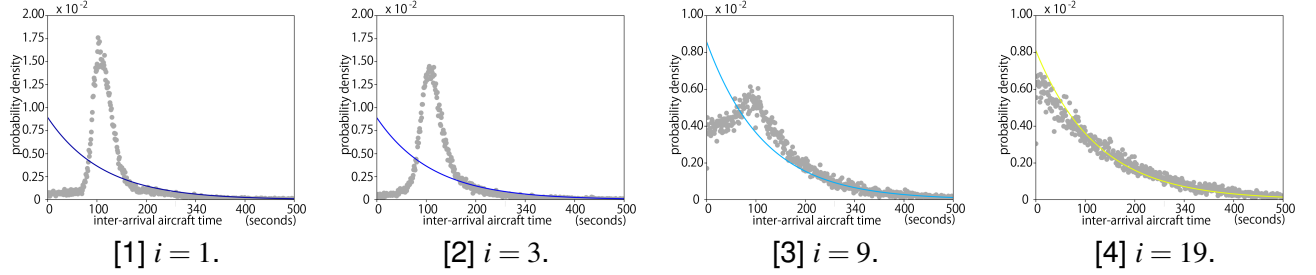[1] $i = 1$.   [2] $i = 3$.   [3] $i = 9$.   [4] $i = 19$.

Figure 5. Distribution of the inter-arrival times with exponential fitting targeting the arrivals at Tokyo International Airport. [2]

International Airport [2]. However, the inter-arrival times converged to a nearly Gaussian distribution toward the departure airports.

Second, the aircraft arrival process at Changi International Airport was analyzed based on the stochastic distribution of the service and inter-arrival times. Airspace $k = 0$ is the area within 10 NM circle, airspace $k = 1$ is the area around the airport in the circular ring defined by the 10 and 20 NM radii, and so on.

Fig. 6 compares the probability distributions of the inter-aircraft time entering each airspace $k \in \{0, 1, 3, 9\}$. The variances of the inter-aircraft time grew more than the actual ones because the ADS-B data does not cover 100% of the arrival traffic due to ADS-B's surveillance limitation. Although these data limitations caused a larger variance than that of the actual traffic, the peak in the distribution disappeared at farther airspaces than $k = 1$. This indicates that the arrival spacing is controlled very close to the airport, approximately around a distance of 10NM from the airport.

To analyze the service times depending on the arrival traffic flows, we categorized the flow by five clusters, as shown in Fig. 7. The first and fifth clusters in Fig. 7 are merged in an en-route airspace, so they were defined as the same traffic group (group 1). The second, third, and fourth clusters were defined as group 2. Then, the probability densities of the service time at airspace $k \in \{1, 3\}$ were compared, as shown in Fig. 8. As depicted in Fig. 8, the mean and variance of the service time in group 2 at $k = 1$ grew. These are the effects of the route designs and arrival operation, which merged the arrival traffic at airspace $k = 1$ right before the approach routes. At airspace $k = 3$, small peaks appeared to increase the service time. As shown in Fig. 2 [2], the flight time is controlled by holding at these airspaces for the arrivals of group 2.

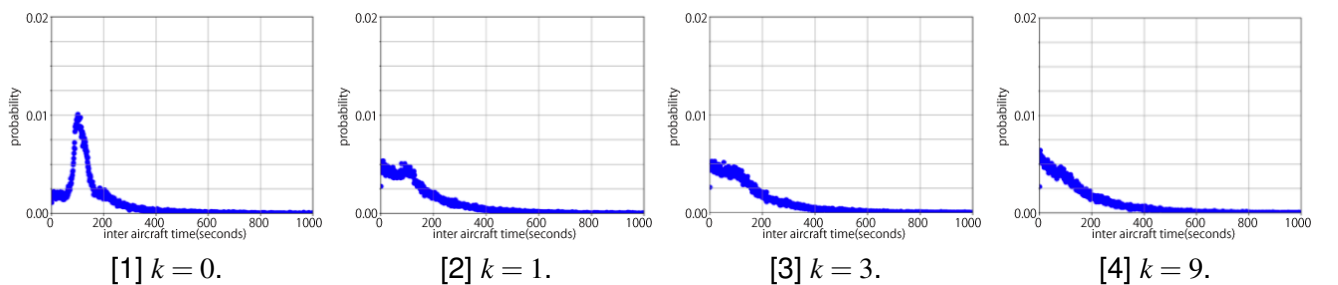[1] $k = 0$.   [2] $k = 1$.   [3] $k = 3$.   [4] $k = 9$.

Figure 6. Distribution of interarrival times targeting the arrivals at Singapore Changi International Airport [6].

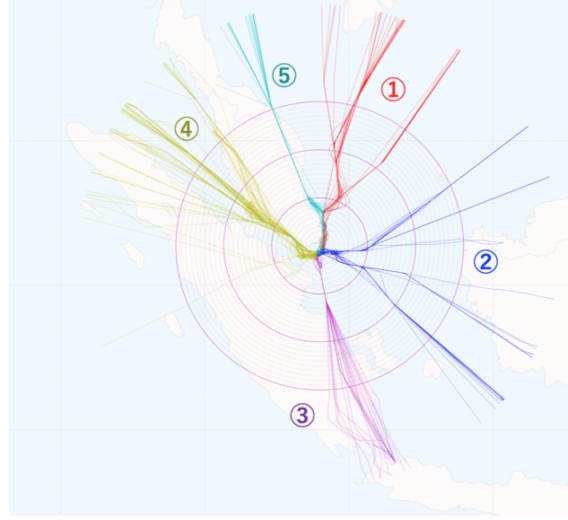Figure 7. One-day examples of the arrival track data with five clusters [6].

[1] $k = 1$, group 1.   [2] $k = 1$, group 2.   [3] $k = 3$, group 1.   [4] $k = 3$, group 2.
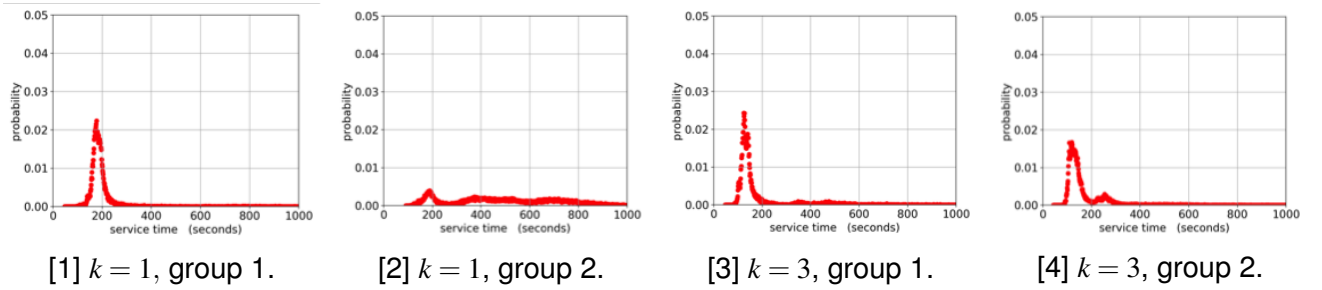
Figure 8. Distribution of the service times for each group targeting the arrivals at Singapore Changi International Airport [6].

3.3 Bottlenecks in the arrival flows

Based on the stochastic characteristics of the inter-arrival time and service time, we modeled the aircraft arrival process in an airspace using the $G/G/c$ models in [2] [3] and the $M/G/c/K$ model in [4]. In this paper, a $G/G/c$ queuing model was briefly described in section 2.2 The $G/G/c$ queuing model allows general distribution for both the service time and inter-arrival time, so it well presents the stochastic features of the aircraft arrival process mentioned above. Here, the bottlenecks in the aircraft arrival traffic at the two case study airports were analyzed based on the balances among the arrival rates, flight times, and capacities, which realize stable arrival flows at assigned airspaces.

First, the maximum arrival rate λ_i, which satisfies the stability conditions (see Eq. (2)) at each airspace i around Tokyo International Airport, was estimated under fixed service rate μ_i, actual data, and airspace capacity $c_i \in \{1, 2, 3\}$, where $\rho \to 1$. Fig. 9 shows the estimated arrival rate in an hour at airspace $i \in \{1, 2, \ldots, 9\}$. As shown in Fig. 9, increasing the airspace capacity c_i allows for higher arrival rates for all of the airspace i. For $c = 1$, 30 arrivals per hour are not allowed because the queue stability condition for airspace $i \in \{1, 2, \ldots, 5\}$ is no longer held. When $c = 2$, the maximum arrival rate allowed in airspace $i = 1$ is 32 arrivals, while 40 arrivals are not allowed in airspace $i = 3$. If $c = 3$, it is possible to have 40 arrivals per hour for all of the airspace.

Tab. 1 summarizes the minimum c_i values for stabilizing the $G/G/c$ model for airspace $i \in \{1, 2, \ldots, 9\}$. This shows that the airspace closer to the airport requires more capacity (large values for c_i), especially in the airspace $i \in \{1, 3\}$. This is because close to the destination airport, i.e., airspace $i = 1$, the aircraft slows down. Thus, the mean service rate is reduced. In the airspaces $i = 3$ and 4, especially $i = 3$, the inter-arrival time is controlled by using vectoring operations. As a result, in this airspace, aircraft change their heading directions and adjust the spacing between succeeding aircraft. Therefore, the service rate μ_i is reduced in the airspaces $i = 1, 3, 4$. In $i = 2$, the aircraft inter-arrival time is already controlled, and most of the arriving aircraft follows in-trail because the airspeed is faster than in the $i = 1$ airspace.
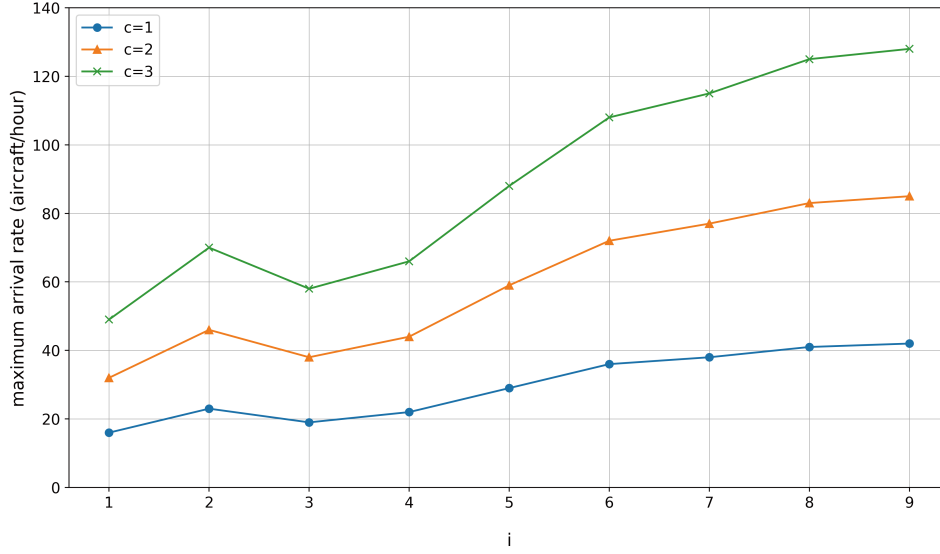
Figure 9. Maximum arrival rate at assigned airspaces around Tokyo International Airport. [3]

TABLE 1. MINIMUM c_i VALUES AT ASSIGNED AIRSPACES AROUND TOKYO INTERNATIONAL AIRPORT. [3]

Arrival rate	Airspace i								
(aircraft / hour)	1	2	3	4	5	6	7	8	9
30	2	2	2	2	2	1	1	1	1
35	3	2	2	2	2	1	1	1	1
40	3	2	3	2	2	2	2	1	1

Next, we applied the analysis to Singapore Changi International Airport. As shown in the previous section, the arrival traffic of group 2 has an impact on the increasing service time (flight time) $\mathbb{E}[B_k]$ at airspace $k = 1$. Also, reducing the service rate $\mu_k = 1/\mathbb{E}[B_k]$ increases ρ_k, which is a key parameter that impacts the $G/G/c$ queuing model, as shown in Eq. (2).

Fig. 10 compares the maximum arrival rate that satisfies the stability condition shown in Eq. (2) when $c = 1, 2, 3, 4, 5, 6$ are given at airspace $k \in \{1, 2, \ldots, 9\}$. In all the given c values, the maximum arrival rate at airspace $k = 1$ is limited compared with the other airspaces. To stabilize the queuing system at airspace $k = 1$, $c \geq 4$ is required when 30 aircraft arrive per hour, and $c \geq 5$ when 40 aircraft arrive per hour. This means that the current arrival strategy at the $k = 1$ airspace requires higher airspace capacity right before the approach phase during congested periods.

Tab. 2 summarizes the minimum capacity value c_k that satisfies Eq. (2). As shown in Tab. 2, the airspace closer to the airport requires more capacity, especially at airspace $k = 1$. By comparing the minimum capacity values c_i in Tab. 1 for the arrivals at Tokyo International Airport, it is obvious that different arrival strategies are given to these case study airports.

The above bottleneck analysis and comparison indicate that designing routes and operational strategies in terminal airspaces needs important rules for conducting stable arrival operations close to destination airports.

4. Effectiveness of the point-merge operation

4.1 Point-merge operation at Tokyo International Airport

Toward even more efficient operation in the terminal airspace surrounding Tokyo International Airport, the PM operation has been implemented into arrival traffic operation since the end of July 2019. Figure 11 compares the flight tracks arriving at Tokyo International Airport in a day before and after the PM implementation. The two major arrival traffic flows enter the terminal area crossing the transition points SPENS and SELNO and following the PM routes in the terminal area, as shown in Fig. 11[2].
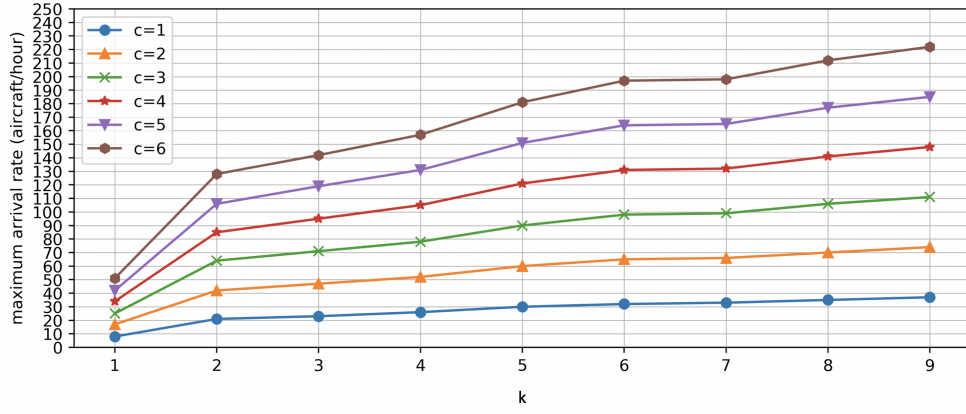
Figure 10. Maximum arrival rate at the assigned airspace around Singapore Changi International Airport [6].

TABLE 2. MINIMUM c_k VALUES AT THE ASSIGNED AIRSPACE AROUND SINGAPORE CHANGI INTERNATIONAL AIRPORT [6].

Arrival rate	Airspace k								
(aircraft / hour)	1	2	3	4	5	6	7	8	9
30	4	2	2	2	1	1	1	1	1
35	5	2	2	2	2	2	2	1	1
40	5	2	3	2	2	2	2	2	2

Figure 12 shows one of the representative PM routes from the southwest direction to RW34L at Tokyo International Airport. The arc of the PM routes was set between 40 NM and 50 NM radius concentric circles centered at the airport's airspace $i = 4$.

This section evaluates the effectiveness of the PM operation using actual flight plans and arrival track data (total 13 days in November and December of 2019) corresponding to the arrival traffic from the southwest region under northerly wind operation during congested time periods, from 5:00 PM to 10:00 PM.

4.2 Analyzing the arrival traffic flow at airspace $i > 5$

This section analyzes the impacts of the PM operation at airspace $i > 5$, in which the arrival traffic flies before entering the PM routes. Figure 13 shows the stochastic distribution of the inter-arrival

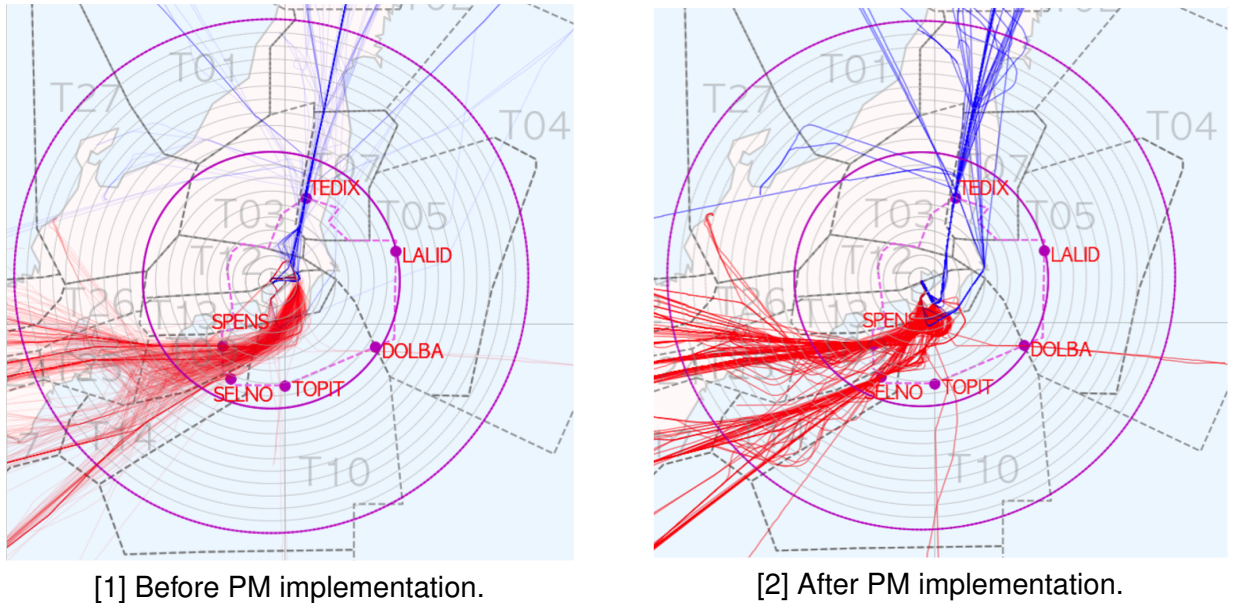[1] Before PM implementation.

[2] After PM implementation.

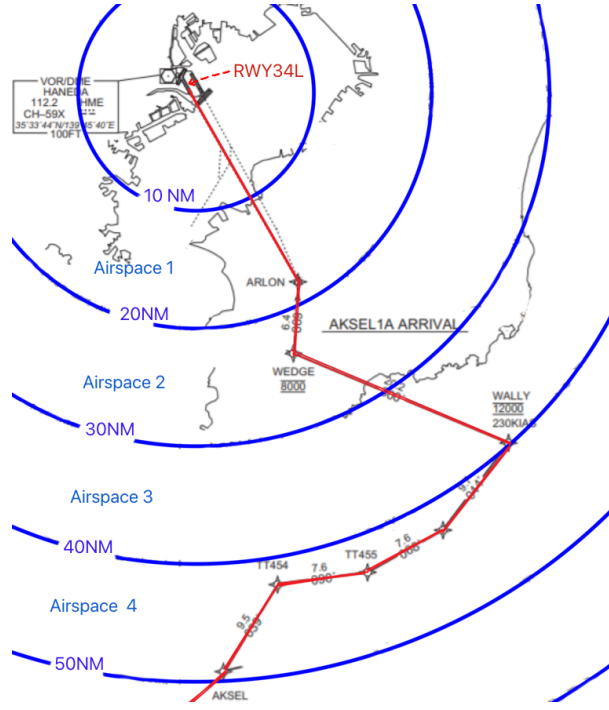Figure 11. Comparing the flight tracks arriving at Tokyo International Airport before and after PM implementation.

Figure 12. One representative PM route from the southwest region to RW34L at Tokyo International Airport.

times at airspace $i \in \{6, 8, 10, 12\}$. As shown in Figs.13 [2] and [3], the deviations of the inter-arrival times are smaller than those of Figs.13 [1] and [4] (having a peak value unlike the exponential distribution) according to the features of the arrival traffic flow before entering the terminal airspace in Fig. 11[2]. Two main streams of the arrival traffic from the southwest region merge at two transition points while keeping in-trail separation and then follow the standard arrival routes (STAR). Once the arrival traffic enters the transition points, the deviation of the inter-arrival times grows (getting close to the exponential distribution) as shown in Fig.13 [1].

Table 3 estimates the arrival delay time at airspace $i \in \{6, 7, 8, 9, 10\}$ using the $G/G/c$ model in Eq.1 when $c_i = 2$ and compares the estimated delay times before and after the PM implementation , under the current arrival rate 30 aircraft in an hour (see Fig. 11[1] and [2]) . According to the growing deviation of the inter-arrival time before entering STAR, the arrival delay time and ρ increased at airspace $i \in \{6, 7\}$ after the PM implementation.

4.3 Estimating the future arrival delays at airspace $i \in \{1, 2, 3, 4, 5\}$

Next, this section estimates the arrival delay times when PM is implemented into the terminal area under the current arrival rate, 30 aircraft per hour (30 ac/hour), and the increasing arrival rate, 35 aircraft per hour (35 ac/hour).

Figure 14 compares the stochastic distributions of the service times at airspace $i \in \{1, 2, 3, 4, 5, 6\}$. The deviation of the service time grew at airspace $i = 4$ according to the location of the arc of the

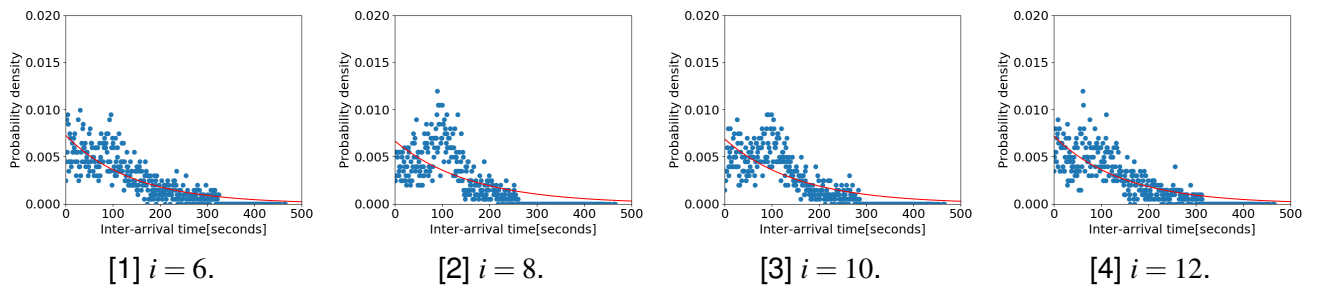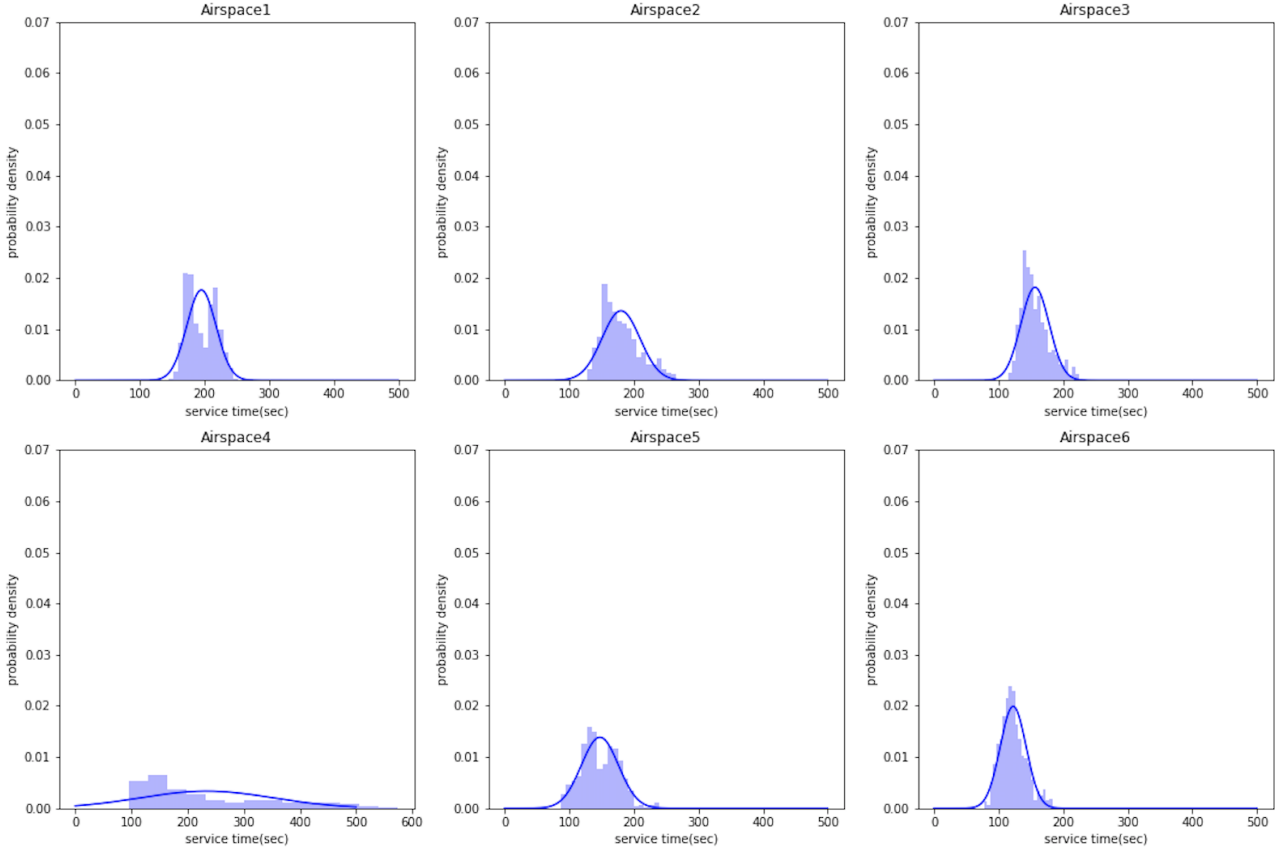| [1] $i = 6$. | [2] $i = 8$. | [3] $i = 10$. | [4] $i = 12$. |

Figure 13. Distribution of the interarrival times at airspace $i = 6, 8, 10, 12$ before entering the PM routes with exponential fitting.

Figure 14. Service time distribution of the arrivals at RW34L in the airspace $i = 1,2,3,4,5,6$ with Gaussian fitting.

PM route, as shown in Fig. 12. The estimated c_i corresponding to airspace $i \in \{1,2,3,5,6\}$ is 2, and $c_i = 3$, where $i = 4$.

Table 4 compares the arrival delay times at airspace $i \in \{1,2,3,4,5\}$ in the cases of 30 and 35 ac/hour. Under the current arrival rate (30 ac/hour), airspace $i = 4$ observes 29.65 seconds. Although the delay time grew under the increasing arrival rate (35 ac/hour) up to 71.76 seconds, the arrival traffic in airspace $i = 4$ was stable, $\rho < 1.0$. To reduce the delay time in airspace $i = 1,2,3$, increasing c_i (reducing aircraft separation) is the solution. For airspace $i = 5$, there are two solutions: increasing c_i and reducing the deviation of the inter-arrival time. To realize deviation reduction, the arrival separation needs to be well-controlled at the upper stream of the arrival traffic flows before entering the PM routes.

5. Conclusion

This paper presented data-driven and theoretical modelings of the arrival traffic flow at Tokyo International Airport and Singapore Changi International Airport. A queue-based modeling based on a stochastic data analysis of the flight (service) time, airspace capacity, and inter-arrival time was established, and it led to better understandings of the characteristics and bottlenecks of air traffic flow. The effectiveness of the PM operation implemented in the terminal areas of Tokyo International Airport

TABLE 3. COMPARISON OF THE ESTIMATED ARRIVAL DELAY TIMES AT AIRSPACE $i = 6,7,8,9,10$ BEFORE AND AFTER THE PM IMPLEMENTATION

	i	6	7	8	9	10
Before PM	ρ	0.4135	0.3883	0.3588	0.3493	0.3419
	$E[D_i^{G/G/c}][\text{sec}]$	2.8	2.5	2.0	2.1	2.2
After PM	ρ	0.5166	0.4305	0.3655	0.3397	0.3223
	$E[D_i^{G/G/c}][\text{sec}]$	8.9	4.9	1.6	1.4	1.3

TABLE 4. ESTIMATING THE ARRIVAL DELAY TIME WITH INCREASING THE ARRIVAL RATE ON THE PM ROUTE.

	i	1	2	3	4	5
	c	2	2	2	3	2
30 ac/hour	ρ	0.8109	0.7494	0.6514	0.6462	0.6160
	$E[D_i^{G/G/c}]$[sec]	25.32	24.48	16.28	29.65	19.00
35 ac/hour	ρ	0.9461	0.8743	0.7600	0.7539	0.7186
	$E[D_i^{G/G/c}]$[sec]	154.5	81.87	40.32	71.76	43.99

was evaluated using data-driven modeling approaches. The arrival delay times at the surrounding airspace of the airport were estimated based on the queuing theory. To improve the efficiency of the PM operation, two strategies were suggested to reduce arrival delay time: 1) reducing the deviation of inter-arrival time before entering PM routes and 2) increasing airspace capacity after flying from PM routes. These results can contribute to the design of operational strategies and requirements that can lead to even better arrival management systems. The airspace capacity close to airports is also a matter of airport operation, which includes departure and surface management. This research extends the proposing approach and aims to establish a scientific and systematic method of designing future ATM systems by integrating data science, theoretical modeling, and simulation evaluation.

6. Acknowledgment

7. Contact Author Email Address

mailto: eriitoh@g.ecc.u-tokyo.ac.jp

8. Copyright Statement

References

[1] Itoh E, Miyazawa Y, Finke M., and Rataj J. Macroscopic Analysis to Identify Stage Boundaries in Multi-Stage Arrival Management. *Air Traffic Management and Systems IV*, Springer Nature, 2021.

[2] Itoh E and Mitici M. Queue-Based Modeling of the Aircraft Arrival Process at a Single Airport. *Aerospace*, 6(10), 103, 2019.

[3] Itoh E and Mitici M. Evaluating the Impact of New Aircraft Separation Minima n Available Airspace Capacity and Arrival Delay. *The Aeronautical Journal*, 124(1274), 447-471, 2020.

[4] Itoh E and Mitici M. Analyzing Tactical Control Strategies for Aircraft Arrivals Using Queue-based Modeling. *Journal of Air Transport Management*, 89(101938), October 2020.

[5] Sekine K, Kato F, Kageyama K, and Itoh E. Data-Driven Simulation for Evaluating the Impact of Lower Arrival Aircraft Separation on Available Airspace and Runway Capacity at Tokyo International Airport. *Aerospace*, 8(6), 165, 2021.

[6] Itoh E, Schultz M, Athota S, and Duong V. Devising Strategies for Aircraft Arrival Processes via Distance-based Queuing Models. *SESAR Innovation Days*, December 2020.

[7] Schultz M, Lubig D, Rosenow J, Itoh E, Athota S, and Duong V. Concept of a Long-Range Air Traffic Flow Management. *SESAR Innovation Days*, December 2020.

[8] Robert C.R and Rosenshine M. The Application of Semi-Markov Decision Processes to Queuing of Aircraft for Landing at an Airport. *Transportation Science*, 19(2), 152-172, 1985.

[9] Bolender M.A and Slater G.L. Evaluation of Scheduling Methods for Multiple Runways. *Journal of Aircraft*, 37(3), 410-416, 2000.

[10] Bäuerle N, Engelhardt-Funke O,and Kolonko M. On the Waiting Time of Aarriving Aircraft and the Capacity of Airports with One or Two Runways. *European Journal of Operational Research*, 177(2), 1180-1196, 2007.

[11] Long D, Johnson J, Gaier E. M, and Kostiuk P. F. Modeling Air Traffic Management Technologies with a Queuing Network Model of the National Airspace System. *NASA Langley Technical Report Server*, 1999.

[12] Adan I and Resing J. Queuing Systems. 2015.

[13] Hillier F. Introduction to Operations Research. *Tata McGraw-Hill Education*, 2012.